Reconstruction of bowing point friction force in a bowed string

J. Woodhouse[a)]
Department of Engineering, Cambridge University, Trumpington Street, Cambridge CB2 1PZ, United Kingdom

R. T. Schumacher[b)] and S. Garoff
Department of Physics, Carnegie Mellon University, Pittsburgh, Pennsylvania

(Received 25 August 1999; accepted for publication 28 March 2000)

A method is presented for reconstructing the friction force and the velocity at the bowing point of a string excited by a rosined bow sliding transverse to the string. Two versions of the method of reconstruction are presented, each approximate in different ways, but both capable of sufficient accuracy to allow useful application to problems of understanding frictional interactions in this dynamical system. The method is illustrated with simulated data to verify its accuracy, and results are shown for two contrasting cases of observed stick-slip string motion. As has been found in other investigations, the friction force during sliding is not determined by the instantaneous sliding speed. The results seem to be compatible with a thermally based model of rosin friction. © *2000 Acoustical Society of America.* [S0001-4966(00)01507-1]

PACS numbers: 43.75.De, 43.40.Cw, 43.60.Pt [WJS]

INTRODUCTION

The excitation of autonomous oscillations in a stretched string by drawing a bow transversely across it is thought to have originated no later than the 10th century.[1] The historical reference to the earliest use in Islamic societies is accompanied by the remark that the ''string'' of the bow, i.e., the horsehair, has been rubbed with ''pitch or resin.'' The bow has been used for musical purposes ever since, most familiarly in the instruments of the violin family. To achieve the characteristic slip-stick oscillations whose nature was first identified by Helmholtz[2] it is necessary to use a substance as an intermediary between string and bow that adheres sufficiently strongly to the string during the sticking part of the motion, and that ''softens'' so as to encourage steady oscillations when the string dynamics breaks the adhesive bond and slipping occurs.

The intermediary substance has conventionally been rosin, a solid distillate obtained from the pitch of coniferous trees. Rosin has extraordinary frictional properties which make it ideal for this purpose. A physically plausible theoretical model for the motion of a bowed string must obviously include a constitutive model for rosin friction. Experimental techniques and theoretical modeling developed for this purpose may have applications in other areas involving stick-slip friction.

The behavior of frictional force and velocity at the contact region of a simple dynamical system excited into stick-slip vibration has been reported by Smith[3] and Smith and Woodhouse.[4] Their system was a version of the prototypical autonomous oscillator system of a system of a single mass on a spring with continuous excitation by a rosin-coated rod moving at constant velocity. Because this system is so simple, it is straightforward to infer the frictional force from observations of the motion of the vibrating mass. The results showed clearly that the frictional force could not be explained with a simple functional relation between the force and velocity, as had been assumed in all previous discussions of rosin-mediated slip-stick motion. An improved constitutive law governing rosin friction is obviously needed. Based on their observations, Smith and Woodhouse[4] proposed models in which friction depends not on sliding speed but on contact temperature.

The oscillator used by Smith and Woodhouse in their measurements necessarily had properties quite different from those of a stretched string. To reconstruct the frictional force and the velocity of a real string at the bowing point from observations of the string's motion is less easy, but a method of doing this was first described by Schumacher.[5,6] We report here a further development of that method, backed by more extensive experimental results. With care, the velocity of a string at the bowed point can be observed directly and noninvasively by the use of a laser-Doppler vibrometer, but there is no corresponding direct method of measuring frictional force. The reconstruction method overcomes the difficulties of direct observation by using the signals from force transducers that serve as the fixed terminations of the string. Both the frictional force and the string velocity at the bow can be deduced from these transducer signals. The approach has the advantage of not disturbing the motion of the string or interfering with the physical properties in the vicinity of the friction contact.

We present first the governing equations, then describe two alternative methods for reconstructing the force and motion at the bowing point. One of the methods allows reconstruction for all motions of the string, including particularly the nonperiodic motions that occur during the initial transient part of the motion. In its present implementation this method is limited by a requirement that the string terminations be effectively rigid. The dispersive effects of propagation along the string are included by a time-domain approach based on

[a)]Electronic mail: jw12@eng.cam.ac.uk
[b)]Electronic mail: rts@andrew.cmu.edu

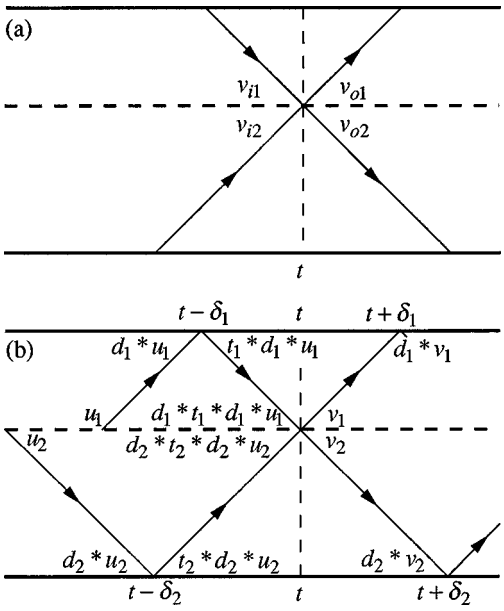

FIG. 1. Space–time diagrams of traveling velocity waves on the string which interact at the bowed point at a particular instant. Horizontal axis: time; vertical axis: distance along the string; horizontal dashed line: bow position; vertical dashed line: required time t. Labeling of trajectories is described in the text.

FIR digital filters. The second method could more readily be applied if the terminations were not rigid, so that their dynamics have an effect on the string's motion. However, this method can only be applied to periodic motions of the string since the crucial stage of the analysis is carried out in the frequency domain. Both methods are limited to excitation by a bow whose dynamics can be neglected. To achieve this in the laboratory we use as a ''bow'' a rosin-coated glass rod rigidly attached to a massive sled that is computer controlled to move in a precisely-defined way.

To illustrate the reconstruction methods, they are applied to measured signals from the experimental system. Some typical results are shown, and their significance discussed. To assess the accuracy of the approach we also apply them to simulated signals, obtained using a model of rosin friction proposed by Smith and Woodhouse[4] and embodying a reasonably accurate representation of the transverse and torsional dynamics of the string used in the experimental tests. In this case the correct velocity and force at the bowed point are known from the simulation, so that a direct assessment of the accuracy of the method is possible.

I. THEORY

Figure 1 shows two space–time (or characteristic) diagrams relating to the trajectories of propagating transverse waves on the string that are relevant to events at the bow (horizontal dashed line) at time t. Time runs horizontally, and position along the string runs vertically. In Fig. 1(a) are shown the two incoming and two outgoing waves, denoted v_{i1}, v_{o1}, v_{i2}, v_{o2}. For an ideal string with tension T and mass per unit length m, these quantities suffice to determine the velocity v and the force f at the bow. The velocity follows by continuity, in the two alternative expressions

$$v = v_{i1} + v_{o1} = v_{i2} + v_{o2}. \tag{1}$$

Corresponding expressions for the force are given by the following argument. In the absence of a force applied at the bow, the two incoming waves would simply carry on unchanged as the outgoing waves. The effect of the applied force is to generate an additional velocity wave which radiates equally in both directions outwards from the bow, thus modifying both outgoing waves relative to the incoming waves. For an ideal string the additional outgoing velocity wave has magnitude $f/2Z$, where

$$Z = \sqrt{Tm} \tag{2}$$

is the wave impedance of the string. It follows that

$$f = 2Z(v_{o1} - v_{i2}) = 2Z(v_{o2} - v_{i1}). \tag{3}$$

Equality of these two expressions is readily shown to be equivalent to equality of the expressions in Eq. (1).

The strategy now is to express the incoming and outgoing velocities at the bow in terms of the forces on the terminations at earlier and later times determined by the propagation times from the terminations to the string. For this we need a larger portion of the characteristic diagram, shown in Fig. 1(b). Following one segment of trajectory some notation can be defined. Consider a velocity wave leaving the bow, denoted u_1 in Fig. 1(b). By the time this wave returns to the bow it has been modified by various linear processes. First, the wave propagates to the end of the string, during which journey some dispersion and dissipation take place. This is represented by convolution with a function d_1, the convolution operator being denoted ''$*$.'' The wave now reflects from the string termination, a process represented by convolution with a function r_1. Finally, the wave propagates back to the bow, represented by a second convolution with d_1. These stages are all labeled in the figure, together with similar sequences for the other initial velocity waves denoted v_1, u_2, v_2. The time delays denoted δ_1, δ_2 are assumed to be incorporated within the definitions of the transmission functions d_1 and d_2.

The forces exerted by the terminations on the string are now

$$f_1(t-\delta_1) = Z(r_1*d_1*u_1 - d_1*u_1), \tag{4a}$$

$$f_1(t+\delta_1) = Z(r_1*d_1*v_1 - d_1*v_1), \tag{4b}$$

$$f_2(t-\delta_2) = Z(r_2*d_2*u_2 - d_2*u_2), \tag{4c}$$

$$f_2(t+\delta_2) = Z(r_2*d_2*v_2 - d_2*v_2). \tag{4d}$$

If the terminations are rigid, these reduce to simpler forms because the reflection process becomes a simple multiplication by -1. Then,

$$f_1(t-\delta_1) = -2Zd_1*u_1, \tag{5a}$$

$$f_1(t+\delta_1) = -2Zd_1*v_1, \tag{5b}$$

$$f_2(t-\delta_2) = -2Zd_2*u_2, \tag{5c}$$

$$f_2(t+\delta_2) = -2Zd_2*v_2, \tag{5d}$$

so that the (measured) force waveforms are equal (apart from a scalar multiplication by $2Z$) to the velocity waveforms sent out from the terminations towards the bow.

Equations (4), or (5) if appropriate, can be used to provide the needed velocities v_{i1}, v_{o1}, v_{i2}, v_{o2} if they can be deconvolved, that is, if they can be solved for the velocities in terms of the measured termination forces. There are two approaches to the problem of eliminating the velocities in favor of the termination forces, depending on whether one works in the time domain or the frequency domain. If the termination is rigid and the dissipation during one transit of a wave between bow and termination is small, then a simple time-domain approach is possible which uses digital filters to effect the solution. In the absence of dissipation on the string, the functions d_1 and d_2 are all-pass filters representing the dispersive propagation on the string. These functions can be represented as FIR digital filters, by virtue of an explicit expression for the propagation of an impulse along a stretched string with nonzero bending stiffness due to Scott, described by Woodhouse.[7] The velocity at position x after time t is given approximately by

$$v(x,t) \approx \frac{3^{1/6}(k_p^2+1)^{2/3}}{2^{2/3}(2k_p^2+3)^{1/2}\bar{t}^{1/3}} \mathrm{Ai}\left[-\left(\frac{3\bar{t}}{2} \right)^{2/3} \frac{k_P^2}{(k_P^2+1)^{1/3}} \right], \tag{6}$$

where Ai is the Airy function, k_p is a stationary-phase wave number satisfying

$$k_P^2 = \frac{1-4\tau^2+(1+8\tau^2)^{1/2}}{8\tau^2}, \tag{7}$$

and

$$\bar{t} = t\frac{T}{\sqrt{Bm}}, \quad \bar{x} = x\sqrt{\frac{T}{B}} \tag{8}$$

are nondimensional time and distance, with $\tau = \tilde{t}/\bar{x}$ and where B is the bending stiffness of the string. In practice, it is necessary to apply an antialiasing low-pass filter to this function, as illustrated by Woodhouse.[7]

Now it is a property of any such all-pass digital filter that its inverse may be obtained simply by time reversal. This reversal is an anticausal filter, which advances the signal in time while ''de-dispersing'' it. This is precisely what we need to obtain the outgoing velocity wave v_1 from the velocity wave at the termination, $d_1 * v_1$, and similarly for v_2 and $d_2 * v_2$. Denote these inverse filters d_1^{-1}, d_2^{-1}. The four velocity waves needed to reconstruct the force and velocity according to Eqs. (1) and (3) are then given by

$$v_{i1} = d_1 * f_1/(2Z), \tag{9a}$$

$$v_{01} = -d_1^{-1} * f_1/(2Z), \tag{9b}$$

$$v_{i2} = d_2 * f_2/(2Z), \tag{9c}$$

$$v_{02} = -d_2^{-1} * f_2/(2Z). \tag{9d}$$

Provided the assumptions of this model are satisfied, these equations give a way to find the velocity and force under the bow from arbitrary waveforms f_1 and f_2, including initial transients. If the assumptions are not satisfied, in particular if the string terminations are sufficiently nonrigid to influence the dynamics of the vibration, then things become more difficult. In principle it might still be possible to design an inverse digital filter to deconvolve the effects of reflections at the terminations, but this is likely to be difficult in practice. If this problem must be grappled with, it is easier to work in the frequency domain, where the operations of convolution and deconvolution are replaced by algebraic operations with transfer functions. The price of this approach is that it can only be implemented robustly when the measured signals f_1 and f_2 are periodic to reasonable accuracy.

For deconvolution in the frequency domain, the data must first be made digitally periodic by resampling it into a form that has an integral number of samples per period over at least a few periods, so that the data excerpt which will be processed is cyclic. Now Eqs. (4) can be Fourier transformed: transforms of each quantity are denoted by corresponding upper-case letters:

$$U_1 = \frac{F_1^{\mathrm{del}}}{ZD_1(R_1-1)}, \tag{10a}$$

$$V_1 = \frac{F_1^{\mathrm{adv}}}{ZD_1(R_1-1)}, \tag{10b}$$

$$U_2 = \frac{F_2^{\mathrm{del}}}{ZD_2(R_2-1)}, \tag{10c}$$

$$V_2 = \frac{F_2^{\mathrm{adv}}}{ZD_2(R_2-1)}. \tag{10d}$$

The superscripts ''del'' and ''adv'' refer to the transforms of $f_j(t-\delta_j)$ and $f_j(t+\delta_j)$, respectively. These expressions are then used in Eqs. (1) and (3) to obtain the expressions for bow force and velocity transforms, which are finally inverse transformed to the time domain.

The limitation on the reflection functions is no longer required, but the reflection functions must nevertheless be known. We will describe in the next section how the transmission functions are obtained from a combination of theory and fitting to plucked data. For our particular apparatus, it was not necessary to determine reflection functions since the terminations were sufficiently rigid to allow reasonable reconstructions assuming perfect delta-function reflection behavior. However, if it were desired to apply the method to bowed strings attached to a real violin body, an additional procedure would be necessary to identify the reflection function. The simplest way to obtain a first approximation to this would be to measure the input admittance at the instrument bridge, and then use a theoretical expression given by Woodhouse [Ref. 7, Eq. (6)]. It should be pointed out that, of course, the frequency-domain method can equally well be applied to rigid-termination data, as is needed by the time-domain method described above, subject to the limitation that a suitably periodic region of the bowed data set can be found.

II. PLUCK TESTS

To accomplish the reconstruction of the events at the bowing point, one needs, in addition to the termination force waveforms, the gains of the two input channels of the force transducers, and accurate values for the time delays from the bowed point to the two terminations. In addition, one needs to know the string's wave impedance, and information about wave dispersion, which is to be expected as a result of the string's bending stiffness. Good estimates of these quantities can be obtained from a calibrated pluck of the string, achieved by breaking a fine wire at the bowing point and recording the subsequent termination signals. The wire we use is 44 gauge copper magnet wire, for which independent measurements have determined that the breaking strength when looped around the string is 1 N, with an uncertainty of about 3%. The string that will provide the illustrations used in this paper is a violin E string, constructed of plain steel wire with no wrappings. In our experiments the string length $L=0.314\,\mathrm{m}$. For a fundamental frequency of 660 Hz, the tension of this string is 72.5 N and the wave impedance is $Z=0.175\,\mathrm{Ns/m}$.

The solid lines in Figs. 2(a) and 2(b) show the measured force signals from a pluck at a distance from the nearest termination of βL where $\beta=0.3$. The growing oscillations that precede each step in the signals show the effect of dispersion. It is easy to compute the theoretical form of such pluck responses, if it is assumed that the wave propagation behavior on each section of the string is governed by transmission functions d_1 and d_2 which are (suitably filtered) versions of the theoretical expression equation (6). The two time delays, the gain factors for the transducers and their amplifiers, and the bending stiffness can all be determined by best-fitting the simulated responses to the measured ones: the result is shown as the dashed lines superimposed on the measurements in Fig. 2. The fit between theory and measurement is generally excellent, giving some confidence in the use of these transmission functions for the deconvolution process. The value of the bending stiffness B was found to be $4.7\times10^{-5}\,\mathrm{N\,m^2}$. This value is in good agreement with expectation: for a circular wire of radius a, the theoretical value is

$$B=\pi E a^4/4, \tag{11}$$

and with $E=210\,\mathrm{GPa}$ and a measured radius $a=0.13\,\mathrm{mm}$, this gives the same result within the measurement uncertainty.

The most obvious area where the signals do not quite agree is just after the first force step in Fig. 2(a) or 2(b): the theory predicts constant force whereas the measurement shows some variation. This is probably evidence of nonrigidity of the termination, so that resonances of the support structure are excited by the step in force. Having determined the transmission functions d_1 and d_2 as above, it might be possible in principle to use the pluck response data to find the reflection functions r_1 and r_2 needed to describe this nonrigidity, by attributing to them the disparity between the theoretical and measured step responses. If the reflection functions are short compared to the reflection times on the string, extraction might be relatively straightforward. However, if the reflection functions involve long reverberation (as they would if the string were mounted on a real violin), the extraction process could be expected to be very tricky. For this initial study the terminations will be assumed to be rigid.

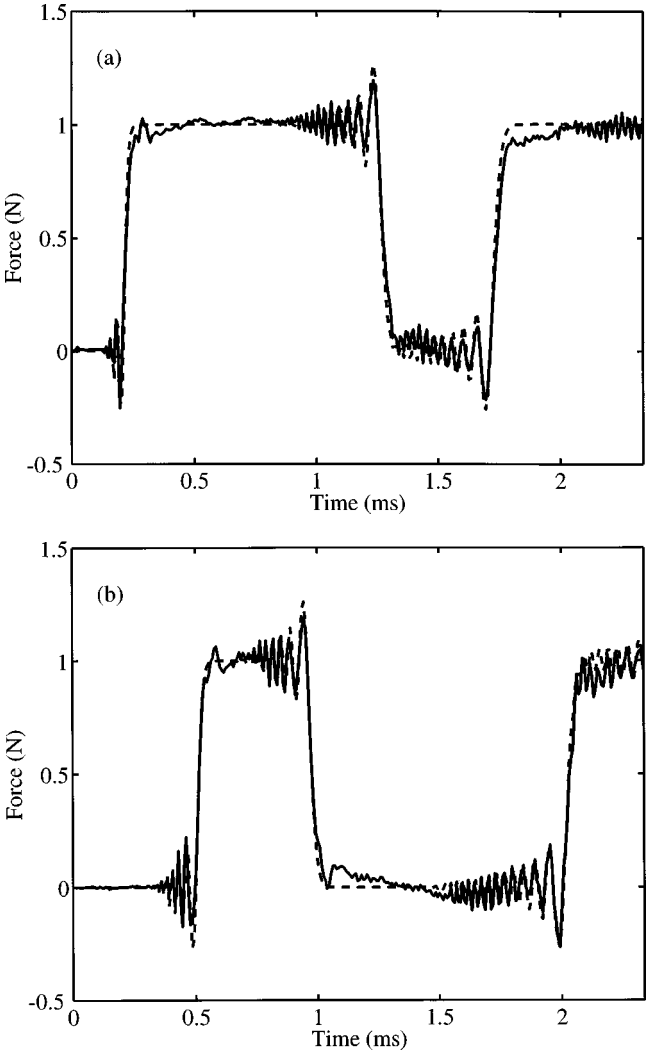

FIG. 2. Measured (solid) and theoretical (dashed) waveforms of force at the string's terminations following a pluck: (a) end nearer to pluck position and (b) end remote from pluck position.

Each time a run is made on the apparatus, a corresponding pluck test is also made. The fitting procedure just described is then used to determine the correct time delays to the ends of the string, and the gain factors for the transducers. This takes into account any variations in string tension, position of bowing point, and transducer performance. The bending stiffness is kept constant at the value stated above, since there is no reason to expect this to vary from day to day with a given steel string.

III. RECONSTRUCTION OF VELOCITY AND FORCE

A. Time-domain reconstruction

Having analyzed the pluck response to obtain the time delays and so on, the time-domain reconstruction of a bowed signal is now straightforward to carry out. Example results will be shown from a run with the bowing point at $\beta=0.3$ as appropriate to the pluck results already shown, with a normal force between rod and string of 0.3 N. The rod was of glass,

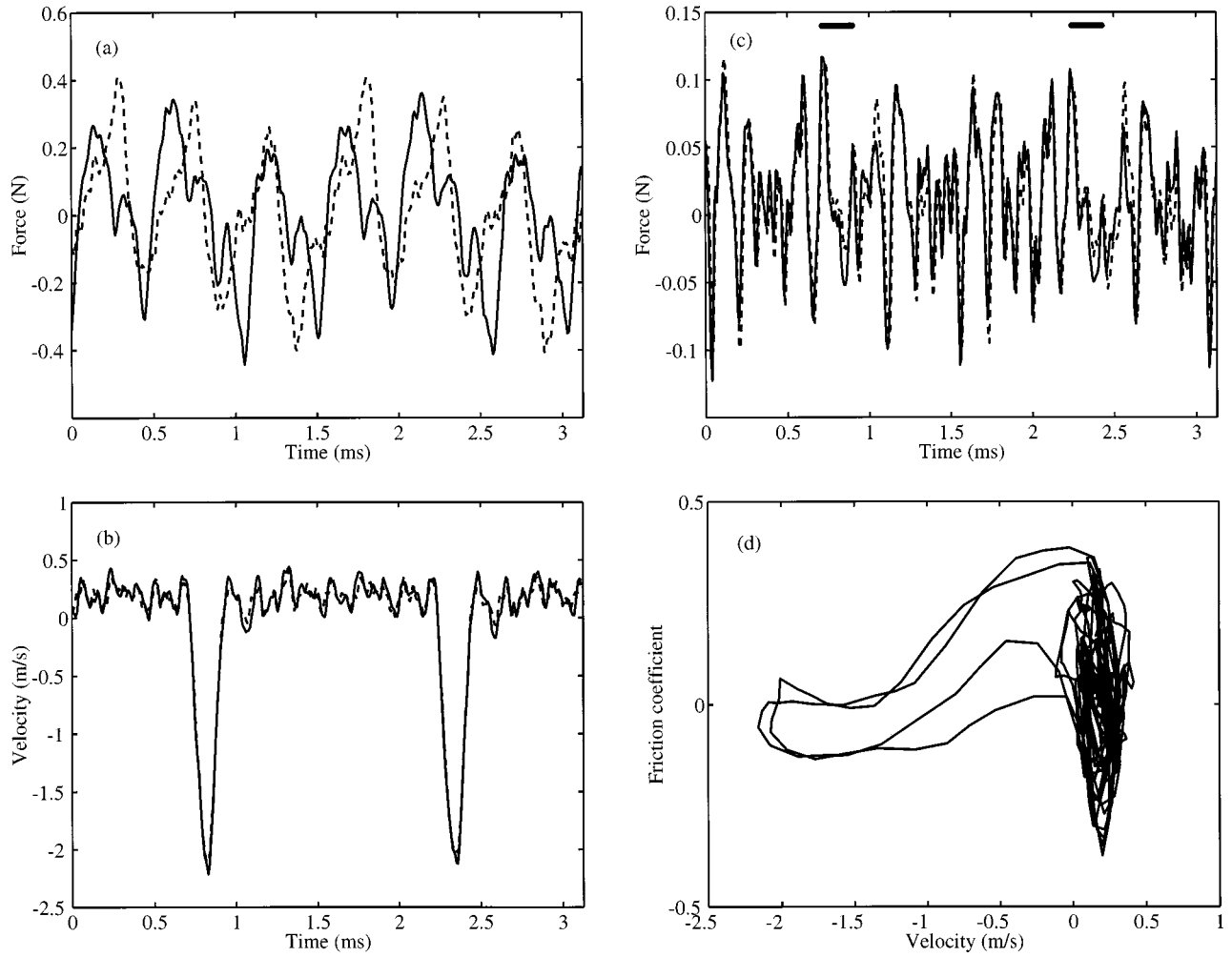

FIG. 3. Results for nearly periodic motion from a typical experimental run with the glass bow: (a) measured forces at the string's terminations; (b) waveforms of the deduced bowing-point velocity from Eqs. (1); (c) waveforms of the deduced bowing-point friction force from Eqs. (3); and (d) velocity/force trajectory of the data shown in (b) and (c). In (c), the segments of heavy horizontal line indicate the times of slipping deduced from (b).

with a diameter of 6 mm and a surface finish smooth to within 5 μm. It was coated not with ordinary violin rosin, which contains unknown chemical impurities, but with technical grade abietic acid, the principal constituent of rosin. The abietic acid was dissolved in ethanol, and the rod was drawn vertically from a container of this solution so that a uniform layer was deposited when the solvent evaporated.

To excite the string into vibration, the rod was driven at a ''bowing'' speed of 0.2 m/s. After a transient, the string settled into a reasonably periodic oscillation regime. A typical portion of the two measured force signals at the terminations is shown in Fig. 3(a). These signals have been digitized at a rate of 128 kHz, with 16-bit resolution. As is not surprising at this very large value of β, the string has not chosen to oscillate in the ''Helmholtz motion'' which violinists usually require.[2] This would involve a single ''corner'' or velocity jump moving on the string, and would result in a sawtooth wave for both termination force signals. Instead, a more complicated regime is established, one of the ''higher types'' analyzed by Raman.[8]

The two versions of the reconstructed velocity signal under the bow, given by Eq. (1), are shown in Fig. 3(b). To produce the best possible versions of these, the calibration results from the pluck test have been fine-tuned: the two time delays and the relative gain of the two sensors have been slightly adjusted by searching in the vicinity of the initial estimates in order to minimize a measure the difference between the two estimates of the velocity. These adjustments are extremely small, within the limits of uncertainty of the calibration procedure using the pluck data, but nevertheless result in a perceptible improvement in the quality of the results.

It is satisfying to see that the two waveforms are very similar, so that the reconstruction process is at least self-consistent. The waveform shows approximately constant velocity, oscillating around the bow speed, for most of each cycle, followed by a short spell of high negative velocity. This may be tentatively interpreted as a stick-slip oscillation, with a single slip per cycle. The measured velocity, which is the transverse velocity of the string's center, is not exactly equal to the bow speed during sticking, due mainly to torsional motion of the string.[9–11] We return to this issue in some detail in Sec. IV. It is possible to check the reconstruction of the string-center velocity waveform by a direct measurement. A small magnet can be positioned close beneath the string at the bowed point. As the (metal) string vibrates,

a voltage is induced across its ends which is proportional to the velocity through the magnetic field.[9] After suitable amplification, this signal can be displayed and compared with the reconstruction. The resolution of this method is limited by noise and by spatial spread of the magnetic field, but within the measurement accuracy the results are indistinguishable from the reconstructed velocity waveform.

The corresponding reconstructed force signal is shown in Fig. 3(c). Again, two versions are shown, corresponding to the two expressions in Eq. (3). Comparing Eqs. (1) and (3), the difference between the two estimates of reconstructed force is the same as the difference of the two reconstructed velocities (apart from a factor $2Z$). Because the variation of force is much less than that of velocity, this difference shows up more clearly in the force plot. Even so, the two curves are very similar, differing only in local details rather than in major features. Note that the amplifiers for the force sensors are ac-coupled, so that the force signal as computed here has a zero dc level. In practice, there must be a nonzero mean friction force opposing the direction of mean sliding—this would give the force a positive dc value in Fig. 3(c). A value for the missing dc level will be estimated shortly. This issue did not arise with the velocity signals, because for a periodic motion the velocity waveform cannot have a nonzero dc value, otherwise the string would have a net displacement after one cycle.

The time range of Fig. 3(c) is identical to that in Fig. 3(b), and it is interesting to note that the intervals of slipping do not stand out to the eye in the force waveform—these intervals are indicated by the heavy lines at the top of the plot. Comparing carefully, it can be seen that the force is high at the start of slipping, and reduces during the period of slipping. This has a striking consequence if the results are plotted in a different way. Until now, virtually all modeling of bowed-string motion has assumed that the friction force is determined by the sliding speed. If we test this idea by plotting force against sliding speed, as in Fig. 3(d), we see that the traditional assumption is not valid: instead of a single curve, the results show a hysteresis loop in a counterclockwise sense. (To produce this plot, the average of the two versions of the reconstructed force and the average of the two velocity reconstructions have been used.) Similar hysteresis loops have been seen in other measurements of rosin friction.[4] It has been suggested that the variable which governs the friction force is not in fact sliding speed, but the rosin temperature in the contact region. Since the contacting bodies have some thermal inertia, changes in temperature lag behind changes in sliding speed, producing a hysteresis loop in the sense observed here.

Figure 3(d) allows us to make a guess at the unknown dc level of the friction force. Since the shape revealed here is very reminiscent of those found in other experiments using rosin,[4] one might expect the absolute level of the coefficient of friction to be comparable. This would be achieved by adding approximately 0.5 to the coefficient of friction, so that it ranges from about 0.4 to 0.9 in the hysteresis loop. That in turn corresponds to adding a dc force of the order of 0.15 N in Fig. 3(c).

The time-domain reconstruction method should work

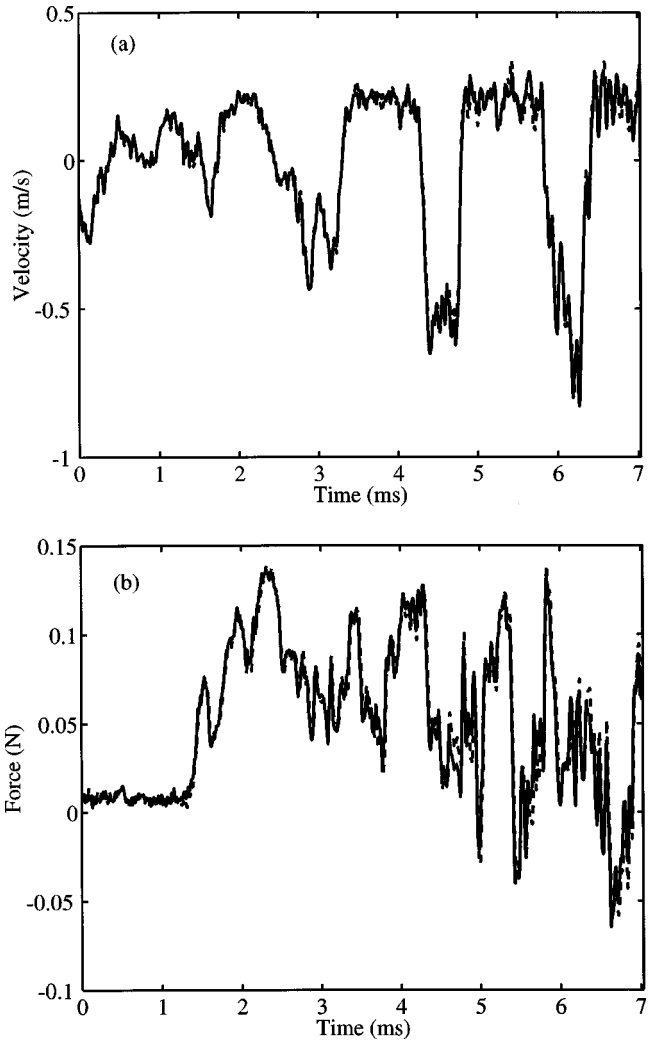

FIG. 4. Results from the initial transient of the experimental run shown in Fig. 3: (a) deduced bowing-point velocity and (b) deduced bowing-point friction force.

equally well during nonperiodic portions of the signal. As an illustration, Fig. 4 shows the reconstructed velocity and force signals from the same experimental run, around the time in the initial transient when the first stick-slip events occur. Again, both versions of the velocity and of the force are shown superimposed. Again, the agreement between the pairs is very good. In this initial stick-slip motion, something closer to the Helmholtz motion is seen: the right-hand half of Fig. 4(a) shows proportions of sticking time to slipping time roughly in the ratio $(1-\beta):\beta$, which is the Helmholtz characteristic. In the nearly periodic data shown in Fig. 3(b), slipping occupied a much smaller fraction of the period. This tendency of Helmholtz motion to be unstable to regimes with shorter slip times, when bowing with large β, has been noted by previous authors.[12,13] This is one reason why in conventional violin playing, β is usually kept rather small except when special effects are wanted.

B. Frequency-domain reconstruction

We now turn to the alternative reconstruction algorithm, operating in the frequency domain. The procedure can be illustrated using the same measured data as shown in Fig. 3.

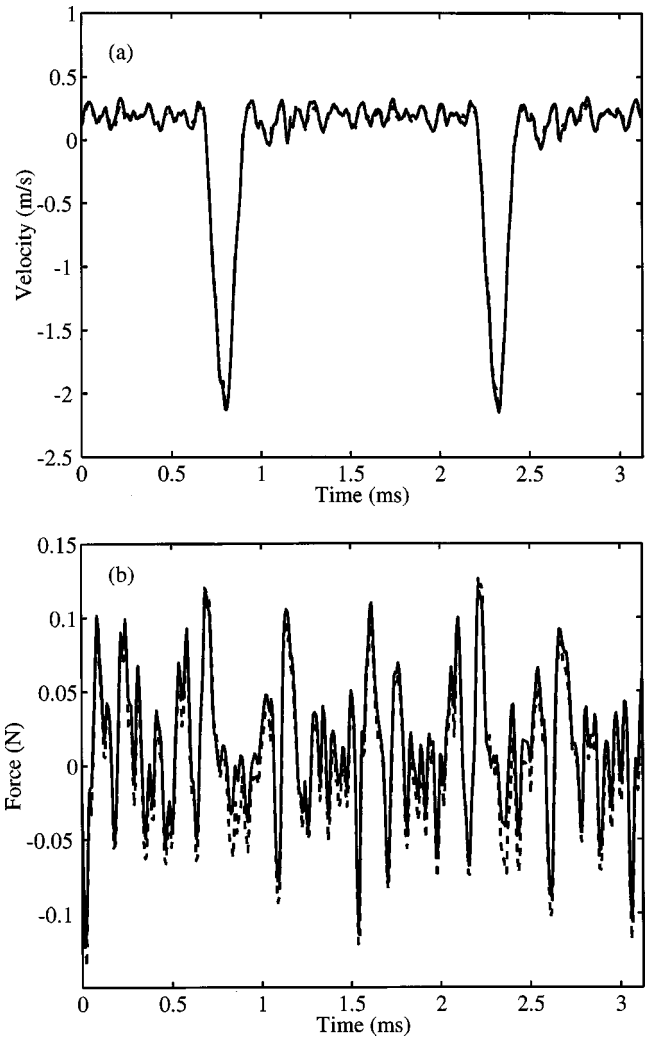

FIG. 5. Comparison of time-domain and frequency-domain reconstruction: (a) deduced bowing-point velocity and (b) deduced bowing-point friction force. Solid lines: time-domain results; dashed lines: frequency-domain results.

As a first stage, the data is resampled so as to produce an integral number of samples per period. For a string adjusted to 660 Hz, the number of samples per period for our sampling rate of 128 kHz is 193.94. A region is selected of about seven periods of the bowed data showing good periodicity. This region is resampled to 200 samples per period, and from that six contiguous periods are selected. Thus the transforms, direct and inverse, are 1200 samples long. The resampling is done by Fourier interpolation. The reconstruction now requires the evaluation of the data at delayed and advanced times. These are not in general integer numbers of samples, so an interpolation scheme is used. Good estimates of the delay times have already been found by analysis of the pluck response. As in the time-domain approach, these can be fine-tuned by a local search during the reconstruction process, to minimize the difference between the two estimates of force (or velocity).

The reconstruction is now carried out using the equations given in Sec. I. Figure 5 shows a comparison between the reconstruction of the bowing force and velocity using the time-domain and frequency-domain methods, for the same section of data shown in Fig. 3. It is very reassuring to see that the two methods give answers which differ from one another by about the same amount as the differences seen in either method separately between the alternative estimates of force and velocity. It seems that whichever way the detailed computation is done, the results are consistent within the bounds shown by Figs. 3 and 5.

C. Reconstruction of simulated data

The next step in assessing the accuracy of the method is to use it to reconstruct signals where the correct answer is known by independent means. The only way to do this at present is to use simulated data. A bowing simulation has been constructed which is reasonably close to the behavior of the physical apparatus as used to generate the results of Figs. 3–5. The general approach to such simulations has been described in detail in previous papers.[14,15] The correct properties were used for the tension, impedance, length, and bending stiffness of the string. Approximately correct Q-factors for transverse modes of the string were included, using a ''constant-Q reflection function'' described in a previous paper.[16] The measured Q-factors for the experimental string were in the range 500–1000 up to 6 kHz, rising to 1000–2000 above that. The model was able to achieve Q-factors around 1000 up 5 kHz, falling gently at higher frequencies to about 600 by 10 kHz because of the filter applied to the stiff-string response, Eq. (6). The bowing speed, normal force and position were matched to the experiment, as was the sampling rate. A plausible model for the torsional behavior of the string was used, with a torsional-to-transverse wave speed ratio of 7, a torsional-to-transverse impedance speed ratio of 3.5, and torsional Q-factors set to a constant value 15 using another version of the constant-Q reflection function.

Finally, the frictional behavior of the rosin was represented by a thermal model described by Smith and Woodhouse.[4] Friction force is regarded as arising from plastic yielding of a thin layer of rosin in the contact region, with a yield strength which varies with temperature in a manner deduced from steady-sliding experiments in a different apparatus.[4] The estimates of the contact size and layer thickness will be discussed in the next section, when the physical evidence of the track left in the rosin surface on the glass rod will be examined. The other thermal properties of rosin were as described in the earlier work. The thermal conductivity of the metal string was assigned a value which was the geometric mean of the values for rosin and steel, to model in a crude way the fact that a layer of rosin is transferred to the string very quickly, and this layer shields the high-conductivity metal from the rapid temperature variations in the thin layer of deforming rosin. This modified value was found to give more realistic results than using the conductivity of steel unmodified.

When this simulation was run, it produced a transient, leading after a while to accurately periodic motion of the string. The transverse forces exerted on the two terminations of the string were stored in the same format as the raw data gathered during the experiments. The simulation program was also used to generate corresponding results of a simu-

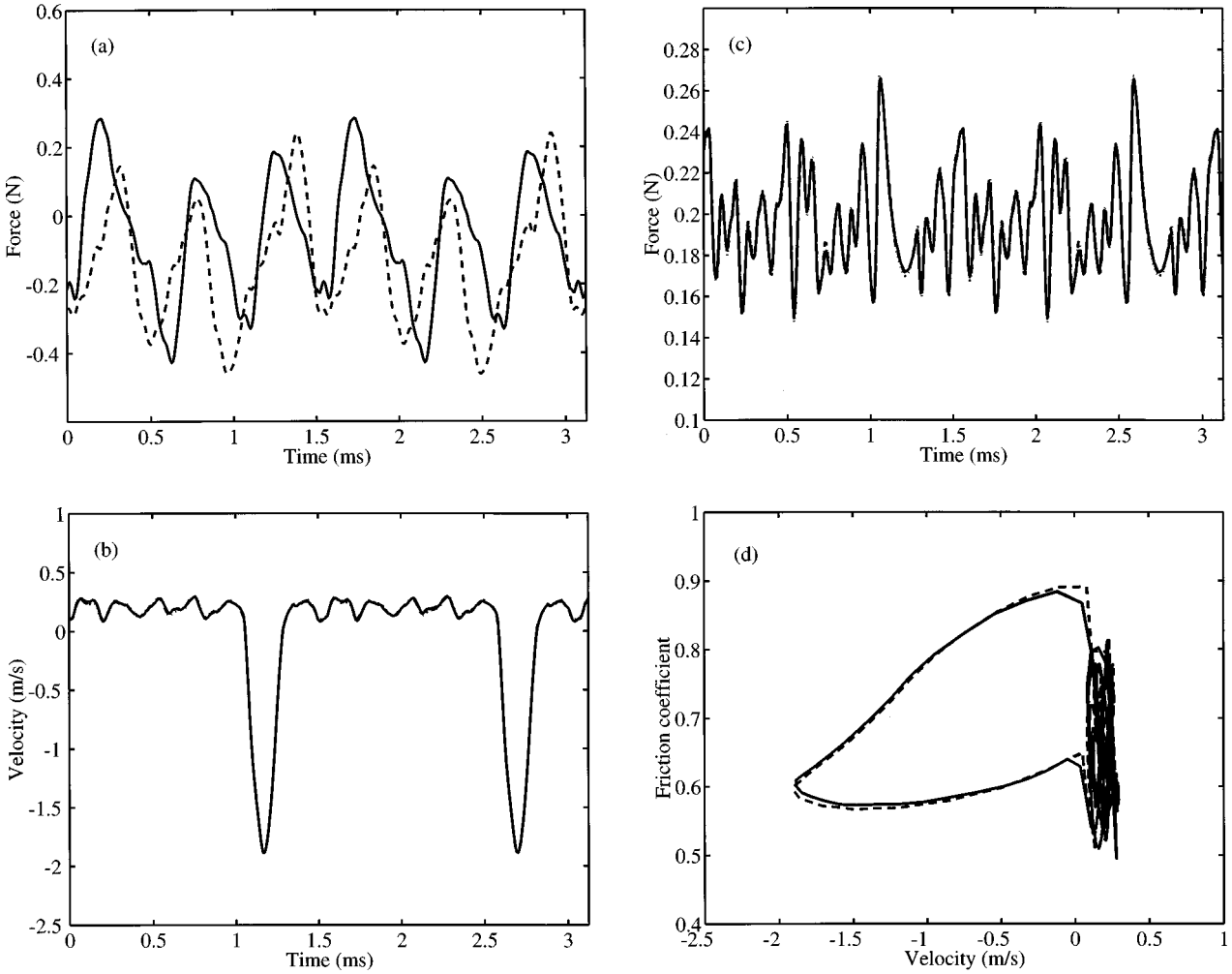

FIG. 6. Results of analysis using simulated bowing-string motion as described in the text, presented in the same form as Fig. 3: (a) forces at the string's terminations; (b) waveforms of the deduced bowing-point velocity from Eqs. (1); (c) waveforms of the deduced bowing-point friction force from Eqs. (3); and (d) velocity/force trajectory of the data shown in (b) and (c). In (b) and (c) the two versions of the deduced waveforms are plotted with solid and dashed lines, while the correct waveforms from the simulation are plotted dotted. In (d) the correct trajectory obtained from the simulation is shown dashed, while the deduced trajectory is shown solid.

lated pluck test. The procedure for time-domain reconstruction of experimental results was then applied, exactly as it was used with experimental data. Results pertaining to the periodic part of the response are shown in Fig. 6, in the same format as those of Fig. 3, with the same axis scalings.

Although it does not particularly matter for the purpose of checking the accuracy of the reconstruction procedure, it is encouraging to see that the simulation has resulted in very similar waveforms to those seen in the experiment. The same regime of oscillation has been chosen by the model string, from among the many which are possible in principle. The ''termination force'' signals, shown in Fig. 6(a), are of similar magnitude and form to those of Fig. 3(a). The reconstructed velocity waveforms, in Fig. 6(b), show stick-slip motion very similar to Fig. 3(b). In the case of the simulation, there is no doubt that the motion really does involve sticking, and that the oscillatory velocity signal seen during the sticking intervals is exactly compensated by torsional motion. Whether this is entirely true for the experimental string will be considered in the next section. The precise form and frequency content of the oscillations during sticking are somewhat different from those in the simulation, which may arise from errors in the assumed friction model or from incorrect values for the torsional properties of the string, especially the frequency-dependent torsional damping, since there is no reliable published measurement of this quantity for any violin E string.

The two versions of the reconstructed velocity waveform from Eqs. (1), shown as solid and dashed lines, also compare well with the exact answer, which was stored during the simulation and is superimposed here as a dotted line. The same is true of the force waveforms, shown with the same plotting conventions in Fig. 6(c). In the simulation, the termination forces have the correct dc level, so that the reconstructed force has a dc level which is missing from Fig. 3(c). Apart from this, the magnitude of the oscillating component of the force is rather bigger for the measured data. However, a careful comparison of Figs. 3(c) and 6(c) shows a very good correspondence of the pattern of major features. In both cases the largest positive value of the frictional force occurs at the onset of slipping, exactly as one would expect

since it is presumably the occurrence of a high force which causes slipping to occur.

As shown by Fig. 6(d), when the reconstructed results are plotted in the force/velocity plane a hysteresis loop is seen, similar to that generated by the measured signals, and circulating in the same counterclockwise sense. The ''correct'' answer from the simulation is shown dashed. This matches the reconstructed version quite accurately. Note that this comparison draws attention to fine details of the force and velocity waveforms during the intervals of slipping only. During sticking, the force fluctuates while the transverse velocity of the string stays approximately constant, resulting in the patch of ''scribble'' to the right of the figure. If the surface velocity, rather than the center velocity, had been used for the horizontal axis, this patch would have appeared as a single vertical line.

These results can be combined with those from the previous section to give a good idea of the overall accuracy of the reconstruction process. A quantitative discussion of this issue requires comparisons between waveforms which are very similar to the eye, so that a numerical measure of difference is required. Various measures are possible, leading to similar conclusions: the following discussion is couched in terms of a normalized rms value of the difference of force waveforms:

$$\Delta = \left[\frac{\Sigma_j (f_j^{(1)} - f_j^{(2)})^2}{\Sigma_j f_j^{(1)^2} + \Sigma_j f_j^{(2)^2}} \right]^{1/2}, \tag{12}$$

where $f_j^{(1)}$ and $f_j^{(2)}$ $(j=1,\ldots,N)$ are the sampled values of the two waveforms being compared. Both waveforms are zero-meaned before this computation. This normalization produces the value unity for uncorrelated signals. Force rather than velocity is chosen because differences are shown more conspicuously, and because the determination of force is the main objective of this study.

By this measure the rms difference between the two versions of the force waveform shown in Fig. 6(c) is $\Delta = 0.07$. When the mean of these two waveforms is compared to the true force from the simulation, the difference is $\Delta = 0.042$. Numbers of this order set a limit to the accuracy which can be expected from the reconstruction method in its current form—the simulated data has no measurement noise, and the underlying dynamical model matches the assumption of the theory used here, so that the differences found here are due to the processing alone. It is, of course, possible that the details of the processing could be improved to reduce these errors further.

The calculated difference of the two force waveforms shown in Fig. 3(c) is $\Delta = 0.20$. It is not surprising to get a bigger difference than for the simulated results, since the experimental results have several additional sources of error: measurement noise, possible misalignment of the two force sensors with respect to the plane of motion, incorrect representation of the transmission function $d(t)$ and its inverse, neglect of the reflection function $r(t)$, and so on. However, one would tentatively conclude from the magnitude of the difference that the mean of the two force estimates might be within 10% or so of the true force. When the comparison is made of the two versions of the force waveform reconstructed by the frequency-domain method, used in Fig. 5, the result is $\Delta = 0.29$. The difference is somewhat bigger than that found with the time-domain method, suggesting that additional errors arise in this approach, probably from noise introduced in frequency ranges where the expressions in the denominators of Eqs. (10) have small magnitude. The time-domain method, in which deconvolution is achieved by the time-reversal trick, does not involve any comparable mechanism of amplifying noise.

IV. RECONSTRUCTION OF TORSIONAL MOTION

The underlying purpose of these experiments is to elucidate the physical mechanisms and behavior of friction at the rod–string contact. It has been shown that the method is capable of giving reasonably convincing versions of the waveforms of friction force and string transverse velocity. However, for a detailed discussion of the micromechanics of friction, the relative motion of the two surfaces is needed. This is somewhat obscured by torsional motion of the string, which cannot be directly observed by the method described here. It would be useful to obtain at least an estimate of the torsional motion.

We can do this by combining the friction force already determined with a theoretical model of torsional response. It is straightforward to convert part of the simulation program used to generate the data of Fig. 6 to this purpose. The average of the two versions of the friction force computed by the time-domain method is taken as the best available estimate of force throughout the transient, and this used as input to a linear model of torsional response. The model operates in the time domain, using constant-Q reflection functions.[16] It should be emphasized at the outset that there is no direct experimental support for this particular form of reflection function for a solid steel string. The most relevant data on torsional behavior of musical strings came from studies of cello strings, which all had a core+wrapping construction. For these strings it was shown that the first few torsional modes were harmonically spaced to reasonable accuracy, and had approximately constant Q-factors.[16] Constant-Q reflection functions give the simplest way to reproduce this behavior.

The model requires as input parameters the torsional wave speed, impedance, and damping. We have reasonable first estimates for the first two of these quantities, based on the standard elastic properties of steel wires. The damping can only be guessed: a number of the order of tens would be consistent with existing data. All these values can be adjusted by searching in the vicinity of the initial estimates, with the aim of minimizing the fluctuation of aggregate velocity, transverse plus torsional, during a typical interval of sticking. If the model were perfect and the string were truly sticking to the rod during these intervals, it should be possible to reduce these fluctuations to zero.

Not surprisingly, it is not possible to achieve this perfect match, but encouraging results can be obtained. The most striking illustration comes from a different experimental run from the one examined so far. When the bowing point was close to $\beta = \frac{1}{4}$, data was obtained which led to a recon-

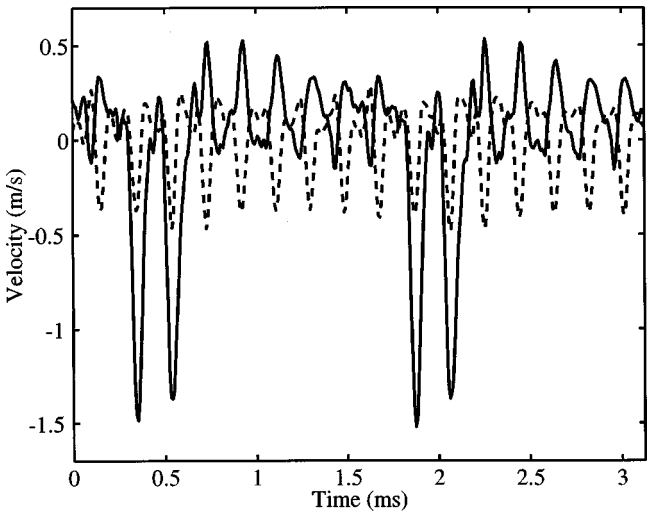

FIG. 7. Reconstructed bowing-point velocity (solid line) and reconstructed surface velocity due to string rotation (dashed line) as described in the text.

structed string-center velocity waveform with unusually large fluctuations of velocity during sticking. A typical portion, where the motion was almost periodic, is shown as the solid line in Fig. 7. The dashed line superimposed on this figure shows the best estimate of the reconstructed torsional motion—it is clear that the waveform is rather close to a mirror image of the transverse velocity during sticking, so that the sum of the two has much smaller fluctuations. In this case, it is easy to believe that at least the majority of the observed velocity fluctuation is caused by torsional motion. The best-fitting torsional wave speed in this case was close to eight times the transverse wave speed, which accounts for the large amplitude of torsional motion. With $\beta=\frac{1}{4}$ the second harmonic of the frequency of ''Schelleng ripples'' [9–11] is approximately in resonance with the fundamental torsional mode. The fitted estimate of torsional speed is consistent with the expected result based on typical handbook values for the density and shear modulus of steel, bearing in mind that the precise values of these quantities are not available for the (unknown) particular steel of this E string.

This procedure for estimating torsional motion using the reconstructed force waveform has been applied to other cases as well. In all cases, the magnitude of the velocity fluctuations during sticking is predicted well, and the detailed motion is matched reasonably well. Also, the best fit is always obtained when the torsional wave speed is around eight times the transverse wave speed, suggesting that this admittedly indirect observation of torsional speed is indeed approximately correct. However, the estimated waveform of torsional velocity should not be regarded as accurate in all details. It is based on a theoretical model, involving the constant-Q reflection functions, for which there is only relatively sketchy validation, and the resonant nature of the torsional waves on the string makes the fine details very sensitive to errors in the friction force waveform. A similar reconstruction can be made for the transverse motion, using the inferred friction force waveform and the corresponding theoretical model for transverse motion. In this case the results can be compared with the known answer, and they turn

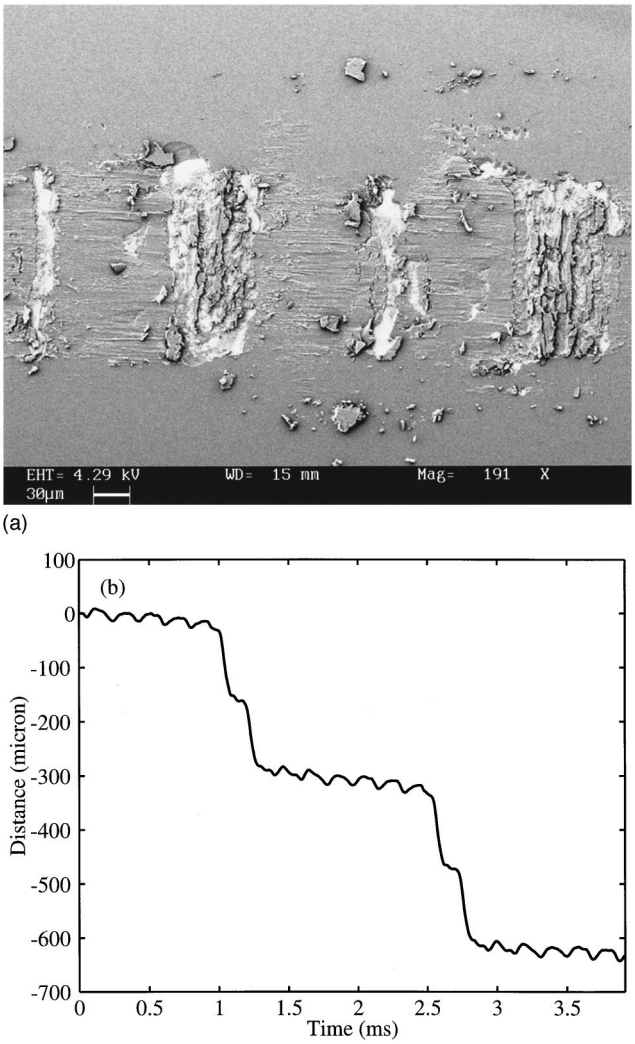

FIG. 8. (a) Scanning electron micrograph of part of the track left in the rosin surface after the bowing run used to compute Fig. 7. (b) Waveform of distance along the glass rod moved by the center of the string during this run, deduced by integration of the solid curve in Fig. 7.

out to be rather poor, presumably because the transverse reverberation time is much longer. It should be noted that the accuracy of the frictional force in this example is probably significantly lower than was the case for the results shown in Fig. 3. When the difference of the two versions of the force is computed the result is $\Delta=0.36$, much larger than the previous case.

We can obtain some further information about the motion in this case by looking at the track left in the rosin surface after the experiment. As has been shown previously,[17] stick-slip events leave tell-tale marks in the rosin. In this case, a section of the rod from the test was coated with a thin layer of gold and examined in a scanning electron microscope. A typical portion of the friction track is shown in Fig. 8(a). The details should be compared with the time history of relative displacement between string and rod, shown in Fig. 8(b), obtained by integration of the difference between the velocity waveform shown in Fig. 7 and the known rod speed. The motion has two slips per cycle, with approximately equal slip distances. These are separated by intervals of sticking which have left conspicuous scars in the

rosin surface. One of the intervals of sticking is very short, leaving a narrow mark each time. The longer interval of sticking involves, as we have just seen, large amplitudes of torsional motion. This has resulted in relatively large scars on the rosin surface, where the material has been churned up. Figure 8(b) also shows that some ''creep'' has occurred during these long intervals of ''sticking:'' the torsional oscillations are superimposed on a nonzero steady velocity difference. The slips show in the picture as relatively smooth surface marked by lines parallel to the slip direction. These are evidence of large deformation in a thin surface layer of the rosin, qualitatively compatible with the theory advanced by Smith and Woodhouse involving shearing of a layer of rosin, generating significant heating in the process.[4]

Much might be learned about the physical mechanisms underlying the friction force deduced by the reconstruction process by examining the details of such friction tracks. Examples can be found of brittle fracture, ductile failure, and delamination failure at, or close to, the rosin/glass interface. Information can be gleaned about the thickness of the rosin layer and of the actively deforming layer during slipping, and about the interaction of torsional motion, heating of the rosin, and creep deformation. These are all topics for later stages of this continuing investigation. For the moment, it is sufficient to deduce from this figure that the reconstructed velocity waveform matches very well, both qualitatively and quantitatively, the pattern of physical traces left in the rosin surface.

V. CONCLUSIONS

A method has been presented for reconstructing the waveforms of friction force and string velocity on a bowed string, at the point of bowing. The method uses measurements of the transverse forces at the two terminations of the string, together with calibration data from the results of a controlled pluck of the string. It has been shown to perform well on simulated signals, where the answer is known in advance. It also performs well, so far as can be established, on real data obtained from a laboratory rig in which a violin E string is bowed with a rosin-coated glass rod. The velocity waveforms obtained by this procedure can be checked by independent methods, and always seem to be reliable. The friction force at the contact point cannot be measured directly, so this procedure provides a totally new source of data to check and refine theoretical models of the process of vibration excitation by friction.

The key feature of the reconstruction method is that the measured force signals must be propagated both forwards and backwards in time and space to establish what happens at the bowed point. Working forwards in time involves convolution with a suitable function to describe the dispersive propagation characteristics of waves on the string. Working backwards involves deconvolution with this function, potentially a more difficult undertaking. Two approaches have been illustrated. The first operates in the time domain and achieves the deconvolution using the fact that if we are only dealing with dispersion and not dissipation, the effect of propagation is represented by an all-pass filter, whose inverse can be obtained by simple time reversal. The second method, which in principle could allow for dissipation and more complicated reflection processes, is carried out in the frequency domain and so is restricted to data which is fairly accurately periodic. Both methods have been shown to work well, and to give consistent answers when both are applicable. For the particular system used in the measurements, the time-domain approach is more versatile.

The results are in good qualitative agreement with measurements of the frictional characteristics of rosin from a different stick-slip oscillator.[4] They show very clearly that the friction force cannot be expressed as a function of the instantaneous relative sliding velocity, a model which has been used almost universally in earlier studies of the motion of a bowed string. When force is plotted against sliding velocity, a hysteresis loop is obtained rather than a single-valued function—an example is shown in Fig. 3(d). It has been suggested[4] that a better model of rosin friction involves the temperature at the contact point. Thermal inertia of the material around the contact results in a time lag between temperature and sliding velocity, which, it is argued, is responsible for the observed hysteresis. Simulation of stick-slip motion using a model based on this idea, together with parameter values appropriate to the experimental rig, produces encouraging qualitative agreement with the measured results (see Fig. 6).

This idea is supported by another aspect of the measurements reported here. After it has been used, once only, in the bowing rig, the glass rod can be examined in the scanning electron microscope. A track is left in the rosin surface which contains a great deal of information about the history of deformation and friction in the rosin layer. An example is shown in Fig. 7(a). Each interval of sticking leaves a conspicuous scar on the rosin surface. During slipping a thin layer of highly-deformed material is visible, as expected from the thermal model. The history of relative displacement between string and rod, revealed by the track, is in good quantitative agreement with that deduced from the velocity waveform.

With this technique we expect to be able to correlate the friction force and the string velocity with position along the friction track and thus correlate the morphology of the interfaces of the wear track with the forces and velocities associated with those events. We will be able to vary both the substrates and the intermediate material—rosin here—to probe how material properties control stick-slip oscillations in this system. This work will lead to a better understanding of the interaction of autonomous dynamical systems and the frictional forces that drive them. We should ultimately be able to provide information which will lead to a more accurate and reproducible production of rosin for bowed-string musical instruments.

ACKNOWLEDGMENTS

The authors thank Claire Barlow and Alan Heaver for their invaluable help with the technology and interpretation of the scanning electron micrograph.

[1] W. Bachmann, *The Origins of Bowing and the Development of Bowed Instruments up to the 13th Century* (Oxford U. P., New York, 1969).

[2] H. Helmholtz, *On the Sensations of Tone* (Dover, New York, 1954).
[3] J. H. Smith, ''Stick-slip vibration and its constitutive laws,'' Dissertation, University of Cambridge, 1990.
[4] J. H. Smith and J. Woodhouse, ''The tribology of rosin,'' J. Mech. Phys. Solids **48**, 1633–1681.
[5] R. T. Schumacher, ''Measurement of bow force,'' Proceeding of the Institute of Acoustics **19**(5), 43–48 (1997).
[6] R. T. Schumacher, ''Studies in bowing-point friction in bowed strings,'' J. Acoust. Soc. Am. **103**, 2915(A) (1998).
[7] J. Woodhouse, ''On the playability of violins. Part I: reflection functions,'' Acustica **78**, 125–136 (1993).
[8] C. V. Raman, ''On the mechanical theory of vibrations of bowed strings,'' Indian Assoc. Cult. Sci., Bull. **15**, 1–158 (1918).
[9] J. C. Schelleng, ''The bowed string and the player,'' J. Acoust. Soc. Am. **53**, 26–41 (1973).
[10] L. Cremer, *The Physics of the Violin* (MIT, Cambridge, MA, 1985).
[11] M. E. McIntyre, R. T. Schumacher, and J. Woodhouse, ''Aperiodicity in bowed-string motion,'' Acustica **49**, 13–32 (1981).
[12] G. Weinreich and R. Caussé, ''Elementary stability considerations for bowed-string motion,'' J. Acoust. Soc. Am. **89**, 887–895 (1991).
[13] J. Woodhouse, ''On the stability of bowed string motion,'' Acustica **80**, 58–72 (1994).
[14] M. E. McIntyre, R. T. Schumacher, and J. Woodhouse, ''On the oscillations of musical instruments,'' J. Acoust. Soc. Am. **74**, 1325–1345 (1983).
[15] R. T. Schumacher and J. Woodhouse, ''The transient behaviour of models of bowed-string motion,'' Chaos **5**, 509–523 (1995).
[16] J. Woodhouse and A. R. Loach, ''Torsional behaviour of cello strings,'' Acustica—Acta Acustica (in press).
[17] R. T. Schumacher and S. Garoff, ''Bowing with a glass bow,'' J. Catgut Acoust. Soc. **3**(2), 9–17 (1996).